VIBRATIONAL BEHAVIOR OF AN ELECTRICALLY ACTUATED MICRO-BEAM WITH THERMOELASTIC DAMPING

A. Karami mohammadi * **N. Ale Ali**

Department of Mechanical Engineering
Shahrood University of Technology
Iran

ABSTRACT

In this paper, a resonator is modeled as a microbeam under the effect of thermoelastic damping and actuated electrically. Two models, small and large deformation models, are represented by considering linear and nonlinear Euler-Bernoulli beam theory. These models are compared against voltage, and the difference between these models is shown and discussed. In the large deformation model, the microbeam deflected due to applied DC voltage, and vibration of microbeam occurs around this static deflection. The vibration equation is linearized around static deflection and by applying harmonic vibration, equation for mode shape and frequency is obtained. The complex frequency is calculated by numerical method and then used for obtaining the Q-factor of thermoelastic damping. The stretching effect and thermoelastic damping is validated with the literature. The result shows that for the high values of voltage, the large deformation model is more accurate. The behavior of thermoelastic damping is also investigated against the geometrical and material properties.

Keywords: Microbeam, resonator, Thermoelastic damping, Electrostatic actuation.

1. INTRODUCTION

In MEMS, there are kinds of damping which affect the performance of the devices. These damping are divided by two parts: a) extrinsic b) intrinsic. Extrinsic damping can be weakened by suitable design, proper methods of fabrication and appropriate operating conditions. For example, squeeze film damping is the extrinsic damping that can be minimized by encapsulating the devices [1,2].

Thermoelastic damping that increases with miniaturization of devices [2], is the intrinsic damping in MEMS. Thermoelastic damping arises from the irreversible heat flux in vibrating structure. Vibration makes part of structure in compression and the other in extension, so the heat flux flows from compressed parts to extended parts. This flux tries to generate the heat equilibrium in the body of structure. The energy used for this equilibrium cannot be stored in the structure so this process is irreversible and entropy generation is occurred. Then some energy is dissipated that is called thermoelastic damping [3].

The first who predicted the thermo-elastic damping was Zener [4,5]. He represented an expression about quality factor of thermoelastic damping in beams. Alblas [6] treated on conversion of mechanical energy into heat in vibrating elastic beam. He obtained an expression that shows this conversion in elastic beam based on linear theory of thermoelasticity. He also found that this damping for macro structures is negligible. Lifshitz and Roukes [7] obtained the quality factor of thermo-elastic beam in micro scale and found that thermoelastic damping in micro and nano scales is important.

For calculating the quality factor of thermoelastic damping, there are two methods: energy method and eigenfrequency method. In energy method, dissipated and maximum stored energy should be calculated (for example see [8,9,11,13]) and in eigenfrequency method, real and imaginary parts of eigenfrequency should be calculated (for example see [2,3,10,12]). Each method can be done with numeric or analytic procedures or combination of them.

Nayfeh and Mohammed [2] modeled the electrostatically microplate by considering thermoelastic damping. They obtained an expression for quality factor analytically by using perturbation. Sun and Saka [3] derived analytical expression of thermoelastic damping for circular microplate. They also obtained a critical thickness for this damping represents the maximum damping. Sudipto and Aluru [8] investigated the thermoelastic damping in electrostatically actuated microbeam by thermal energy method. They studied the effect of applied voltage on thermoelastic damping. Prabhakar and Vengallatore [9] presented an exact theory for thermoelastic damping with 2-D heat conduction. They used Green's function method to solve 2-D heat conduction equation and then derived an expression for quality factor of this damping by calculating the eigenvalues for doubly clamped beam in the form of infinite series.

In MEMS, there are different actuation and sensing

* Corresponding author (akaramim@yahoo.com)

DOI : 10.1017/jmech.2014.12
Copyright © 2014 The Society of Theoretical and Applied Mechanics, R.O.C.
https://doi.org/10.1017/jmech.2014.12 Published online by Cambridge University Press

properties such as thermal, optical, electrostatic, electromagnetic, piezoresistive and piezoelectric but electrostatics is often preferred [26]. In electrostatics an elastic conductor is located above a stationary conductor. The electrical load is composed of two components, including AC and DC voltage. The applied DC voltage deforms the upper elastic surface that causes to change in the system capacitance and to stretch the mid-plane of the elastic surface. The applications are transistors, switches, micro-mirrors, pressure sensors, micro-pumps, moving valves and micro-grippers which have no harmonic motion in their systems. If AC voltage is added to DC one, then resonators are obtained which have harmonic motion [14].

There are many works and papers that investigated the electrical actuation in micro structures. Batra and *et al*. reviewed them in [14]. In his review, many works of Nayfeh and *et al*. are seen [15-23]. In one of them, Nayfeh and *et al*. [15] presented a nonlinear model of electrically actuated microbeams considering mid-plane stretching. They showed the static deflection of the microbeam due to dc polarization and vibration of the microbeam around its statically deflected position.

Also Mohammed has many works that is also explained in [14]. Recently, Hassen and Mohammed [24] investigated the dynamic behavior of clamped-clamped micromachined arches when actuated by a small DC electrostatic load superimposed to an AC harmonic load. They derived a Galerkin-based reduced-order model and utilized to simulate the static behavior and the eigenvalue problem under the DC load actuation. They calculated the natural frequencies and mode shapes of the arch for various values of DC voltages and initial rises.

Accordingly MEMS resonators are devices that vibrate with AC voltage around the static deflection that is due to DC polarization voltage. The thermoelastic damping as well as frequency of structure of resonator is affected by the DC voltage because the thermoelastic damping is directly related to imaginary part of frequency. In addition, in MEMS resonators, high sensitivity and resolution are needed [1] so for achieving this purpose, the damping in such devices should be decreased. However, studying the behavior of thermoelastic damping in resonators is necessary for manufactures of MEMS.

In this paper, a resonator is modeled as a microbeam under the effect of thermoelastic damping and actuated electrically. Two models, small and large deformation models, are represented by considering linear and nonlinear Euler-Bernoulli beam theory. These models are compared against voltage. In this comparison the difference between these models is shown and discussed. In the large deformation model, the microbeam deflected due to DC applied voltage and vibration of microbeam occurs around this static deflection. The vibration equation is linearized around static deflection and by applying harmonic vibration, equation for mode shape and frequency is obtained. The complex frequency is calculated by numerical method and then used for obtaining the Q-factor of thermoelastic damping. The stretching effect and thermoelastic damping is validated with Nayfeh [15] and Lifshitz [7], respectively. The result shows that for the high values of voltage, the large deformation model is more accurate and the behavior of thermoelastic damping is also investigated against the geometrical and material properties.

2. MODELING

The resonator, the Fig. 1, is modeled as a microbeam bending under the electrostatic load which is DC voltage (polarization voltage) V_p. This electrostatic load that is uniform along the width of microbeam is applied by a uniform parallel electrode lying under the microbeam. The microbeam is also clamped at the both ends. $w(x, t)$ is defined as transverse deflection of the beam. Vibration equation of nonlinear thermo-elastic beam considering mid-plane stretching (large deformation) is derived by adding thermal moment, M^T, and thermal axial force, N^T, in "Nonlinear 2-D Euler-Bernoulli Beam Theory" with stretching effect which is presented in [27].

$$\rho A\frac{\partial^2 w}{\partial t^2}+EI\frac{\partial^4 w}{\partial x^4}+\frac{\partial^2 M^T}{\partial x^2}=\frac{\partial^2 w}{\partial x^2}\left\{P(t)-\frac{1}{L}\int_0^L\left[\left(N^T-\frac{\partial M^T}{\partial x}\frac{\partial w}{\partial x}\right)-\frac{EA}{2}\left(\frac{\partial w}{\partial x}\right)^2\right]dx\right\}+\frac{1}{2}\epsilon b\frac{V_p^2}{(d-w)^2} \tag{1}$$

where

$$M^T=E\alpha_T b\int z\theta dz \tag{2}$$

$$N^T=E\alpha_T b\int \theta dz \tag{3}$$

where $\theta=T-T_0$ in which $T(x, z, t)$ and T_0 are defined as temperature field of the beam and stress-free temperature (in equilibrium) respectively. Also, t, α_T, E, $P(t)$, L, b, d, ϵ and ρ are time, coefficient of thermal expansion, Young's modulus, applied axial force, length,

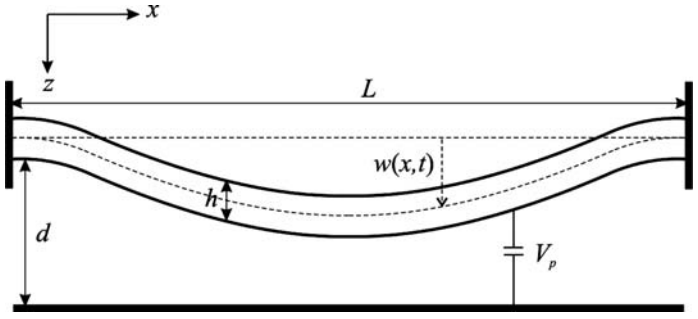


Fig. 1 Schematic of electrically actuated resonator

https://doi.org/10.1017/jmech.2014.12 Published online by Cambridge University Press

width, the gap distance, the dielectric constant and the material density, respectively. It is noted that the cross section of the microbeam is rectangular, thus the area and moment of inertia of the cross section are $A = bh$ and $I = bh^3/12$ where h is the thickness.

The thermal conduction equation, containing the thermoelastic coupling term, can be written as following [7].

$$k\nabla^2\theta + \kappa\frac{\partial^2\theta}{\partial z^2} = \rho c_v\frac{\partial\theta}{\partial t} - \beta T_0 z\frac{\partial}{\partial t}\left(\frac{\partial^2 w}{\partial x^2}\right) \tag{4}$$

where c_v and κ are the specific heat at constant volume and the thermal conductivity, respectively. $\beta = E\alpha_T/(1-2\nu)$ is the thermal modulus where ν is the Poisson ratio. In this model, Lifshitz and (4) can be ignored. Thus the equation is simplified.

Roukes [7] assumption is used. So the thermal gradient in the z direction is much larger than gradient in x and y directions, therefore $\kappa\nabla^2\vartheta$ in Eq. (4) can be ignored. Thus the equation is simplified.

$$\kappa\frac{\partial^2\theta}{\partial z^2} = \rho c_v\frac{\partial\theta}{\partial t} - \beta T_0 z\frac{\partial}{\partial t}\left(\frac{\partial^2 w}{\partial x^2}\right) \tag{5}$$

So the Eqs. (1) and (5) represent the governing equations of nonlinear vibration of micro-beam with thermo elastic damping (TED). In addition, thermal and elastic properties are independent from temperature and the temperature change due to thermoelastic damping is assumed small thus the vibration of micro-plate is investigated in constant temperature, in this case this temperature is considered T_0.

For convenience, the nondimensional variables is introduced (denoted by hats)

$$\hat{w} = \frac{w}{d},\ \hat{x} = \frac{x}{L},\ \hat{t} = \frac{t}{\bar{t}},\ \hat{z} = \frac{z}{h},\ \hat{\theta} = \frac{\theta}{\bar{\theta}} \tag{6}$$

where $\bar{t} = \sqrt{\dfrac{\rho bhL^4}{EI}}$ and $\bar{\theta} = \dfrac{\beta T_0\, dh^3}{\kappa\bar{t}L^2}$. Substituting Eq. (6) into Eqs. (1) and (5), the following equation is obtained

$$\begin{aligned}&\frac{\partial^2\hat{w}}{\partial\hat{t}^2} + \frac{\partial^4\hat{w}}{\partial\hat{x}^4} + \alpha_1\frac{\partial^2\hat{M}^T}{\partial\hat{x}^2}\\ &= \frac{\partial^2\hat{w}}{\partial\hat{x}^2}\left\{\hat{P}(t) - \int_0^1\left[\alpha_6\hat{N}^T - \alpha_2\frac{\partial\hat{M}^T}{\partial\hat{x}}\frac{\partial\hat{w}}{\partial\hat{x}} - \alpha_3\left(\frac{\partial\hat{w}}{\partial\hat{x}}\right)^2\right]d\hat{x}\right\}\\ &\quad + \alpha_4\frac{V_p^2}{(1-\hat{w})^2}\end{aligned} \tag{7}$$

$$\frac{\partial^2\hat{\theta}}{\partial\hat{z}^2} = \alpha_5\frac{\partial\hat{\theta}}{\partial\hat{t}} - \hat{z}\frac{\partial}{\partial\hat{t}}\left(\frac{\partial^2\hat{w}}{\partial\hat{x}^2}\right) \tag{8}$$

where

$$\begin{aligned}&\alpha_1 = \frac{12\alpha_T\bar{\theta}L^2}{hd},\ \alpha_2 = \frac{12\alpha_T\bar{\theta}d}{h},\ \alpha_3 = \frac{6d^2}{h^2},\\ &\alpha_4 = \frac{6\epsilon L^4}{Eh^3d^3},\ \alpha_5 = \frac{\rho c_v h^2}{\bar{t}\,\kappa},\ \alpha_6 = \frac{12L^2\alpha_T\bar{\theta}}{h^2}\end{aligned} \tag{9}$$

$$\hat{M}^T = \int_{-\frac{1}{2}}^{\frac{1}{2}}\hat{z}\hat{\theta}d\hat{z},\ \hat{N}^T = \int_{-\frac{1}{2}}^{\frac{1}{2}}\hat{\theta}d\hat{z},\ \hat{P}(t) = \frac{L^2}{EI}P(t) \tag{10}$$

Boundaries of beam are as following

$$w(0,t) = w(L,t) = 0,\ \left.\frac{\partial w}{\partial x}\right|_{(0,t)} = \left.\frac{\partial w}{\partial x}\right|_{(L,t)} = 0 \tag{11}$$

$$\hat{w}(0,\hat{t}) = \hat{w}(1,\hat{t}) = 0,\ \left.\frac{\partial\hat{w}}{\partial\hat{x}}\right|_{(0,\hat{t})} = \left.\frac{\partial\hat{w}}{\partial\hat{x}}\right|_{(1,\hat{t})} = 0 \tag{12}$$

3. VIBRATION AROUND STATIC DEFLECTION

3.1 Large Deformation Model

The microbeam deflection has two components. The first one, denoted by $\hat{w}_s(\hat{x})$, is due to DC voltage and the second one, denoted by $\hat{v}(\hat{x},\hat{t})$, is due to AC voltage. Thus $\hat{w}(\hat{x},\hat{t})$ can be written as

$$\hat{w}(\hat{x},\hat{t}) = \hat{w}_s(\hat{x}) + \hat{v}(\hat{x},\hat{t}) \tag{13}$$

To calculate the static deflection of the microbeam, the damping concept becomes meaningless so the Eq. (8) is ignored and the time derivatives and the ac forcing term are set zero in Eq. (7). Thus, for achieving the static deflection with clamped-clamped boundaries the following equations are obtained

$$\frac{d^4\hat{w}_s}{d\hat{x}^4} = \frac{d^2\hat{w}_s}{d\hat{x}^2}\left\{\hat{P}(t) + \int_0^1\alpha_3\left(\frac{d\hat{w}_s}{d\hat{x}}\right)^2 d\hat{x}\right\} + \alpha_4\frac{V_p^2}{(1-\hat{w}_s)^2} \tag{14}$$

$$\hat{w}_s(0) = \hat{w}_s(1) = 0,\ \left.\frac{d\hat{w}_s}{d\hat{x}}\right|_{\hat{x}=0} = \left.\frac{d\hat{w}_s}{d\hat{x}}\right|_{\hat{x}=1} = 0 \tag{15}$$

The equation describing the vibration of microbeam around the static deflection is obtained by substituting Eq. (13) into Eqs. (7) and (8) and dropping the terms representing the equilibrium position that is also static deflection (Eq. (14)) and high order terms. The result is written as

$$\begin{aligned}&\frac{\partial^2\hat{v}(\hat{x},\hat{t})}{\partial\hat{t}^2} + \frac{\partial^4\hat{v}(\hat{x},\hat{t})}{\partial\hat{x}^4} + \alpha_1\frac{\partial^2\hat{M}^T}{\partial\hat{x}^2}\\ &= \frac{\partial^2\hat{w}_s(\hat{x})}{\partial\hat{x}^2}\left\{\int_0^1\left[-\alpha_6\hat{N}^T + \alpha_2\frac{\partial\hat{M}^T}{\partial\hat{x}}\frac{\partial\hat{w}_s(\hat{x})}{\partial\hat{x}}\right.\right.\\ &\quad \left.\left. + 2\alpha_3\frac{\partial\hat{w}_s(\hat{x})}{\partial\hat{x}}\frac{\partial\hat{v}(\hat{x},\hat{t})}{\partial\hat{x}}\right]d\hat{x}\right\}\\ &\quad + \frac{\partial^2\hat{v}(\hat{x},\hat{t})}{\partial\hat{x}^2}\left\{\hat{P}(t) + \int_0^1\alpha_3\left(\frac{\partial\hat{w}_s(\hat{x})}{\partial\hat{x}}\right)^2 d\hat{x}\right\}\\ &\quad + \frac{2\alpha_4 V_P^2}{\left(1-\hat{w}_s(\hat{x})\right)^3}\hat{v}(\hat{x},\hat{t})\end{aligned} \tag{16}$$

https://doi.org/10.1017/jmech.2014.12 Published online by Cambridge University Press

$$\frac{\partial^2\hat{\theta}}{\partial\hat{z}^2}=\alpha_5\frac{\partial\hat{\theta}}{\partial\hat{t}}-\hat{z}\frac{\partial}{\partial\hat{t}}\left(\frac{\partial^2\hat{v}}{\partial\hat{x}^2}\right) \tag{17}$$

In this case, the boundaries are obtained as

$$\hat{v}(0,\hat{t})=\hat{v}(1,\hat{t})=0\,,\ \left.\frac{\partial\hat{v}}{\partial\hat{x}}\right|_{(0,\hat{t})}=\left.\frac{\partial\hat{v}}{\partial\hat{x}}\right|_{(1,\hat{t})}=0 \tag{18}$$

Assuming a harmonic vibration in the *n*th mode shape in the form

$$\hat{v}(\hat{x},\hat{t})=\sum R_n(\hat{x})\,e^{i\Omega_n\hat{t}}\ ,\ \hat{\theta}(\hat{x},\hat{z},\hat{t})=\sum\Theta_n(\hat{x},\hat{z})\,e^{i\Omega_n\hat{t}} \tag{19}$$

where Ω_n is the frequency and $R_n(\hat{x})$ and $\Theta_n(\hat{x},\hat{z})$ are the *n*th mode shapes of the beam and the associated temperature variation respectively. Equation (19) are substituted into the (16), (17), (10) and (18).

$$\begin{aligned}&-\Omega_n^2R_n(\hat{x})+\frac{\partial^4R_n(\hat{x})}{\partial\hat{x}^4}+\alpha_1\frac{\partial^2\hat{M}_n^T}{\partial\hat{x}^2}\\&=\frac{\partial^2\hat{w}_s(\hat{x})}{\partial\hat{x}^2}\left\{\int_0^1\left[-\alpha_6\widehat{N}_n^T+\alpha_2\frac{\partial\hat{M}_n^T}{\partial\hat{x}}\frac{\partial\hat{w}_s(\hat{x})}{\partial\hat{x}}\right.\right.\\&\left.+2\alpha_3\frac{\partial\hat{w}_s(\hat{x})}{\partial\hat{x}}\frac{\partial R_n(\hat{x})}{\partial\hat{x}}\right]d\hat{x}\Bigg\}\\&+\frac{\partial^2R_n(\hat{x})}{\partial\hat{x}^2}\left\{\hat{P}+\int_0^1\alpha_3\left(\frac{\partial\hat{w}_s(\hat{x})}{\partial\hat{x}}\right)^2d\hat{x}\right\}\\&+\frac{2\alpha_4V_P^2}{\left(1-\hat{w}_s(\hat{x})\right)^3}R_n(\hat{x})\end{aligned} \tag{20}$$

$$\frac{\partial^2\Theta_n(\hat{x},\hat{z})}{\partial\hat{z}^2}=i\Omega_n\,\alpha_5\Theta_n(\hat{x},\hat{z})-i\Omega_n\hat{z}\frac{\partial^2R_n(\hat{x})}{\partial\hat{x}^2} \tag{21}$$

$$\hat{M}_n^T=\int_{-\frac{1}{2}}^{\frac{1}{2}}\hat{z}\Theta_n(\hat{x}\,,\hat{z})\,d\hat{z}\ \ ,?\ \hat{N}_n^T=\int_{-\frac{1}{2}}^{\frac{1}{2}}\Theta_n(\hat{x}\,,\hat{z})\,d\hat{z} \tag{22}$$

$$R_n(0)=R_n(1)=0\,,\ \left.\frac{\partial R_n(\hat{x})}{\partial\hat{x}}\right|_{\hat{x}=0}=\left.\frac{\partial R_n(\hat{x})}{\partial\hat{x}}\right|_{\hat{x}=1}=0 \tag{23}$$

For solving Eq. (21), some boundary conditions are needed. These boundary conditions are $\partial\Theta_n/\partial\hat{z}=0$ at $\hat{z}=\pm1/2$ because the upper and lower surfaces of the beam are adiabatic and there is no flow heat across those surfaces. Then solving Eq. (21), yields

$$\Theta_n(\hat{x},\hat{z})=\frac{1}{\alpha_5}\frac{\partial^2R_n(\hat{x})}{\partial\hat{x}^2}\left(\hat{z}-\frac{\sin(N_n\hat{z})}{N_n\,cos(N_n/2)}\right) \tag{24}$$

where

$$N_n=(1-i)\sqrt{\frac{\Omega_n\alpha_5}{2}} \tag{25}$$

Substituting (24) into (22), it is obtained

$$\hat{M}_n^T=C_n^T\frac{\partial^2R_n(\hat{x})}{\partial\hat{x}^2} \tag{26}$$

$$\hat{N}_n^T=\frac{1}{\alpha_5}\frac{\partial^2R_n(\hat{x})}{\partial\hat{x}^2}\left[\frac{\hat{z}^2}{2}+\frac{\cos(N_n\hat{z})}{N_n^2cos(N_n/2)}\right]_{-\frac{1}{2}}^{\frac{1}{2}}=0 \tag{27}$$

where

$$C_n^T=\frac{1}{12\alpha_5}\left[1+f(\Omega_n)\right] \tag{28}$$

$$f(\Omega_n)=\frac{24}{N_n^3}\left(\frac{N_n}{2}-\tan\left(\frac{N_n}{2}\right)\right) \tag{29}$$

Substituting (26) and (27) into (20) the equation of mode shapes and frequencies is obtained

$$\begin{aligned}&-\Omega_n^2R_n(\hat{x})+(1+\alpha_1C_n^T)\frac{\partial^4R_n(\hat{x})}{\partial\hat{x}^4}\\&=\frac{\partial^2\hat{w}_s(\hat{x})}{\partial\hat{x}^2}\left\{\int_0^1\left[\alpha_2C_n^T\frac{\partial\hat{w}_s(\hat{x})}{\partial\hat{x}}\frac{\partial^3R_n(\hat{x})}{\partial\hat{x}^3}\right.\right.\\&\left.+2\alpha_3\frac{\partial\hat{w}_s(\hat{x})}{\partial\hat{x}}\frac{\partial R_n(\hat{x})}{\partial\hat{x}}\right]d\hat{x}\Bigg\}\\&+\frac{\partial^2R_n(\hat{x})}{\partial\hat{x}^2}\left\{\hat{P}+\int_0^1\alpha_3\left(\frac{\partial\hat{w}_s(\hat{x})}{\partial\hat{x}}\right)^2d\hat{x}\right\}\\&+\frac{2\alpha_4V_P^2}{\left(1-\hat{w}_s(\hat{x})\right)^3}R_n(\hat{x})\end{aligned} \tag{30}$$

Applying the finite difference method the frequencies and mode shapes can be determined numerically. In this method, the initial guess is important for converging to correct response. Here, the frequencies and mode shapes of linear clamped-clamped microbeam are considered as the initial guess. Ω_n is a complex value. By separating the real and imaginary parts the Q-factor of thermoelastic damping can be calculated.

$$Q^{-1}=2\left|\frac{\lambda_n}{\omega_n}\right| \tag{31}$$

where the ω_n and λ_n are the real and imaginary part of Ω_n respectively.

In this section, large static deformation due to DC voltage is considered (Eqs. 14 and 15), then vibration about this large static deformation is investigated (Eqs. 16 to 30). This model is named "large deformation model".

3.2 Small Deformation Model

The small deformation model of thermoelastic beam is obtained as following.

$$\hat{x}_j=j\Delta\hat{x}\ \ j=0,1,\ldots,m\ \ \Delta\hat{x}=\frac{1}{m} \tag{32}$$

The above equation is coupled with Eq. (8) through $\hat{M}^T$. In this model, the large static deflection due to electrostatic load is not considered in calculating the

https://doi.org/10.1017/jmech.2014.12 Published online by Cambridge University Press

thermoelastic damping, despite the large deformation. For calculating the thermoelastic damping the below equation should be solved for Ω_n. This equation is obtained by considering harmonic vibration and solved numerically for calculating the thermoelastic damping through Eq. (31).

$$\left(\frac{\partial(.)}{\partial\hat{x}}\right)_m = \frac{(.)_{m+1}-(.)_{m-1}}{2\Delta\hat{x}} \tag{33}$$

where γ_n is obtained by solving the below equation which is got by applying the clamped-clamped boundary condition (12).

$$\left(\frac{\partial^2(.)}{\partial\hat{x}^2}\right)_m = \frac{(.)_{m+1}-2(.)_m+(.)_{m-1}}{(\Delta\hat{x})^2} \tag{34}$$

For $n = 1$, γ_1 is obtained 4,7300. The Eq. (38) has nonlinear term, $f(\Omega_n)$, so this equation is solved by iteration method. The first guess, for starting the solution, is obtained by solving the equation which is got by ignoring nonlinear terms.

In the model introduced by Eq. (37), small static deformation is assumed. This model is named "small deformation model".

4. FINITE DIFFERENCE FORMULATION

The finite difference method is applied for solving Eqs. (14) and (30). In the mesh

$$\left(\frac{\partial^3(.)}{\partial\hat{x}^3}\right)_m = \frac{(.)_{m+2}-2(.)_{m+1}+2(.)_{m-1}-(.)_{m-2}}{2(\Delta\hat{x})^3} \tag{35}$$

partial derivatives in Eqs. (14) and (30) are substituted by their difference approximation [28]

$$\left(\frac{\partial^4(.)}{\partial\hat{x}^4}\right)_m = \frac{(.)_{m+2}-4(.)_{m+1}+6(.)_m-4(.)_{m-1}+(.)_{m-2}}{(\Delta\hat{x})^4} \tag{36}$$

$$\frac{\partial^2\hat{w}}{\partial\hat{t}^2}+\frac{\partial^4\hat{w}}{\partial\hat{x}^4}+\alpha_1\frac{\partial^2\hat{M}^T}{\partial\hat{x}^2} = \frac{\varepsilon bL^4}{2EId^3}V_P v(t)+\alpha_4 V_P^2\hat{w} \tag{37}$$

The above equation is coupled with Eq. (8) through $\hat{M}^T$. For calculating the thermoelastic damping the below equation should be solved for Ω_n.

$$\Omega_n^2 = \gamma_n^4\left[\frac{\alpha_1}{12\alpha_5}\left[1+f(\Omega_n)\right]+1\right]-\alpha_4 V_P^2 \tag{38}$$

where γ_n is obtained

$$\begin{vmatrix}\sin(\gamma_n)-\sinh(\gamma_n) & \cos(\gamma_n)-\cosh(\gamma_n)\\ \cos(\gamma_n)-\cosh(\gamma_n) & \sin(\gamma_n)+\sinh(\gamma_n)\end{vmatrix} = 0 \tag{39}$$

Because of nonlinear terms, the unknowns in each point m, are calculated by iteration. At the first, the large static deflection is obtained by solving the Eqs. (14) and (15) by above discretizations and then the fundamental frequency is calculated by solving the Eqs. (30) and (23) by the same discretization.

5. COMPARISON BETWEEN SMALL AND LARGE DEFORMATION MODELS

The large deformation model of thermoelastic damping of beam which is presented in this paper should be compared with small deformation model.

In MEMS resonators, the beam is deflected by electrostatic load. In this way, in Fig. 2, thermoelastic damping is illustrated versus V_p by both small and large deformation models for silicon microbeam whose properties are listed in Table 1. As can be seen in this figure, for lower values of V_p the models are coincided but for higher values of V_p the thermoelastic damping quantities are different for small and large deformation models. If V_p, as an electrostatic load, is set by large value, the large deformation is occurred and nonlinear properties come out and the small deformation loses its accuracy. Therefore, in higher values of V_p which can influence the nonlinear deformation, the large deformation assumption should be considered for obtaining the thermoelastic damping, otherwise, the small deformation model, Eq. (37), is adequate for obtaining the thermoelastic damping in small values of V_p.

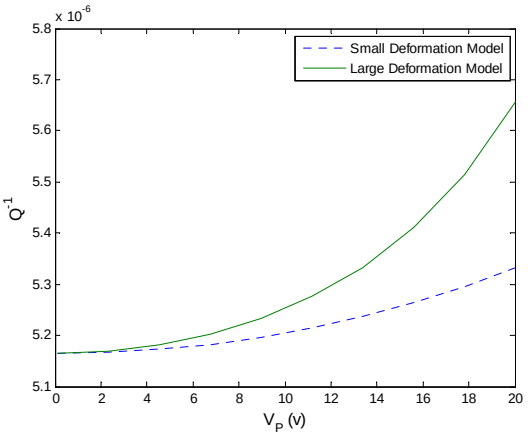


Fig. 2 Comparison of small and large deformation models considering $h = 5\mu m$

Table 1 properties of silicon microbeam [3]

T_0 (K)	E (GPa)	ρ (kg m^{-3})	ν	κ (Wm^{-1}K^{-1})	c_v (Jkg^{-1}K^{-1})	h (μm)
293	165.9	2330	0.22	156	713	5
α_T (10^{-6}K^{-1})	$\hat{P}$	ε (C^{2}m^{-2}N^{-1})	d (μm)	L (μm)	b (μm)	
2.59	0	8.85×10^{-12}	2	700	5	

https://doi.org/10.1017/jmech.2014.12 Published online by Cambridge University Press

6. RESULTS

All the following results are investigated based on the properties of table 1 and by large deformation model. For validation of mid-plane stretching effect the result is compared with reference [15]. Figure 3 shows this comparison. In this comparison, there is not effect of thermoelastic damping and initial stretching. Therefore the α_1, α_2, α_5 and $\hat{P}$ are set zero.

A comparison is made between the small and large deformation and Lifshitz models [7] without electrostatic load based on properties of microbeam listed in Table 1. The comparison is shown in Fig. 4 which is validated the thermoelastic damping effect. This figure shows good agreement between these models.

The thermoelastic damping and fundamental natural frequency are depicted against thickness of microbeam in Figs. 5 and 6, respectively. As can be seen in the Fig. 5, by increasing the thickness, the thermoelastic damping is increased, and for the different values of voltages has the same behavior. Both Figs. 6(a) and 6(b) shows that as thickness increases, the fundamental frequency increases but in different range. The range of the frequency for small value of the voltage, $V_p = 0.1$, is smaller than the range frequency in large value of the voltage $V_p = 20$.

The thermoelastic damping and fundamental natural frequency are depicted against length of microbeam in Figs. 7 and 8, respectively. As can be seen in the Fig. 7, by increasing the length, the thermoelastic damping is decreased, and for the different values of voltages has the same behavior. Both Figs. 8(a) and 8(b) shows that as length increases, the fundamental frequency decreases but in different range. The range of the frequency for small value of the voltage, $V_p = 0.1$, is smaller than the range frequency in large value of the voltage $V_p = 20$.

Figure 9 shows the thermoelastic damping against the gap distance. By increasing the gap distance, the thermoelastic damping is decreased but the rate of this decreasing depends on the V_p, as a electrostatic load. In the high values of electrostatic load this rate becomes sharper and the range of variation is also larger. The variations of the fundamental natural frequency with gap distance are shown in Fig. 10. In this figure, the frequency for lower voltage (Fig. 10(a)) has smaller range than for higher vltage.

Figure 11 shows the variation of thermoelastic damping against Young's modulus. According to this figure, the relation between thermoelastic damping and Young's modulus is approximately linear. As can be seen in Fig. 12 that shows the variations of the fundamental natural frequency with Young's modulus, Young's modulus increases the frequency but for high value (Fig. 12(b)) of V_p, the variation of the frequency is more than the variation of small value of V_p.

The variation of thermoelastic damping against coefficient of thermal expansion is shown in Fig. 13. The thermal moment, that has the main effect in thermoelastic damping by coupling with conduction equation, relates to coefficient of thermal expansion directly. Therefore, as can be seen in Fig. 13, the thermoelastic damping is increased by increasing the coefficient of thermal expansion. According to Fig. 14 that shows the variations of the fundamental natural frequency with coefficient of thermal expansion, this parameter can not affect the frequency because coefficient of thermal expansion is related to thermal moment that affects the thermoelastic damping directly.

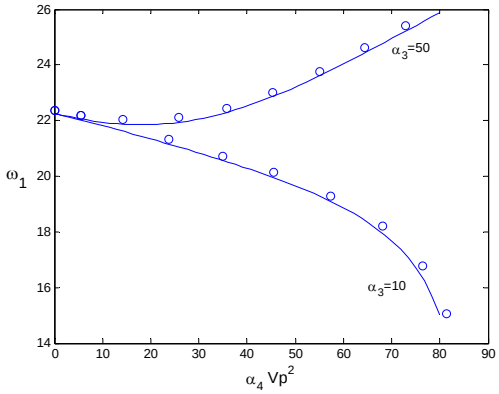


Fig. 3 The fundamental natural frequency using our model (—) compared with the results calculated by reference [15] (o), for $a_3 = 10$ and $a_3 = 50$

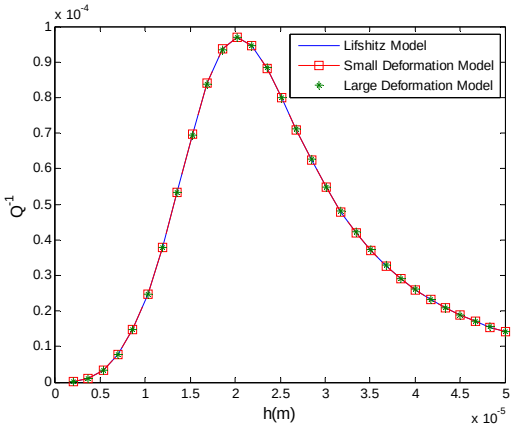


Fig. 4 Comparison small and large deformation and Lifshitz [7] models without electrostatic load

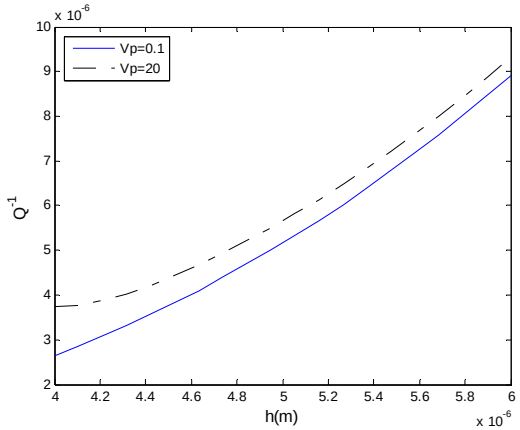


Fig. 5 Thermoelastic damping versus thickness

https://doi.org/10.1017/jmech.2014.12 Published online by Cambridge University Press

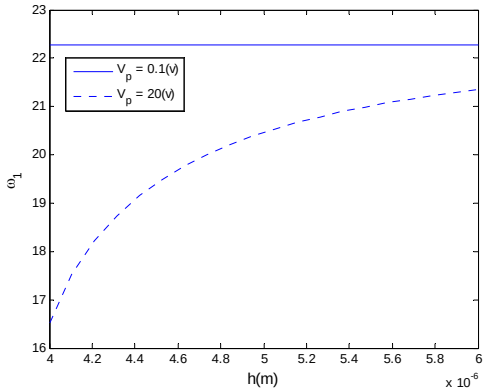


Fig. 6 Variations of the fundamental natural frequency with thickness

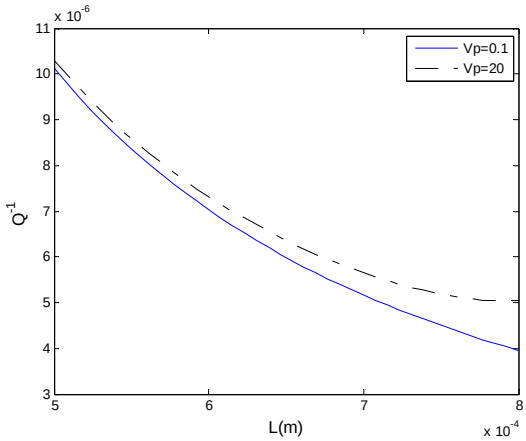


Fig. 7 Thermoelastic damping versus length

7. CONCLUSIONS

In this paper, a MEMS resonator is modeled as a microbeam which is actuated electrically and is under the thermoelastic damping effect. The model involves some nondimensional parameters. Behavior of Q-factor of thermoelastic damping and fundamental natural frequency of microbeam was investigated numerically, with respect to polarization voltage, thickness, length, gap distance, Young's modulus and coefficient of thermal expansion.

The results show that for high values of voltage the large static deflection is occurred in microbeam, for obtaining the thermoelastic damping and frequency, the large deformation model is more accurate than small deformation model in which the nonlinear static deflection is not considered. The geometrical properties can affect the thermoelastic damping. In high values of voltage, the thermoelastic damping has more sensitivity against the gap distance. In high voltage, the fundamental frequency has more range of variation. Increasing the values of Young's modulus and coefficient of thermal expansion can increase the thermoelastic damping. Also Increasing the value of Young's modulus can increase the frequency but coefficient of thermal expansion have no effect on the frequency as a thermal property of material.

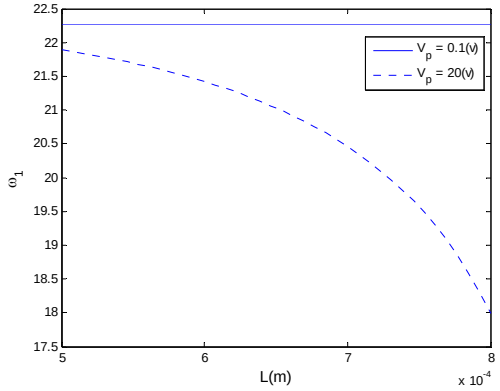
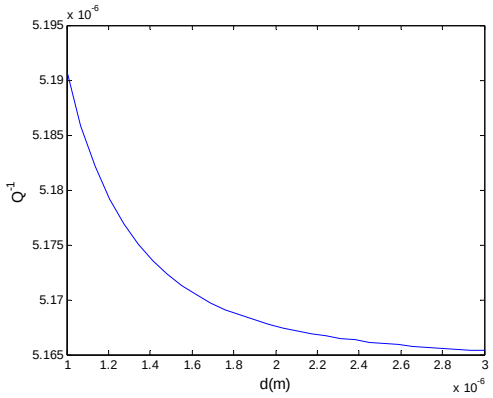
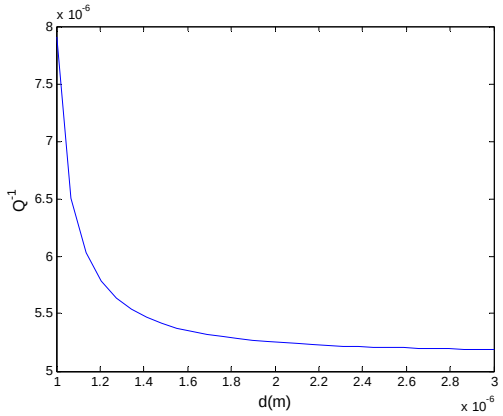


Fig. 8 Variations of the fundamental natural frequency with length



(a)



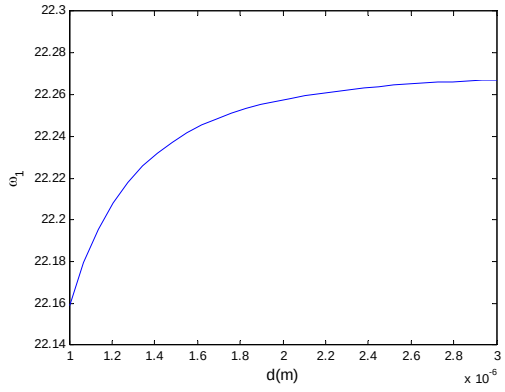
(b)

Fig. 9 Thermoelastic damping versus gap distance (a) $V_p = 2$ (b) $V_p = 10$

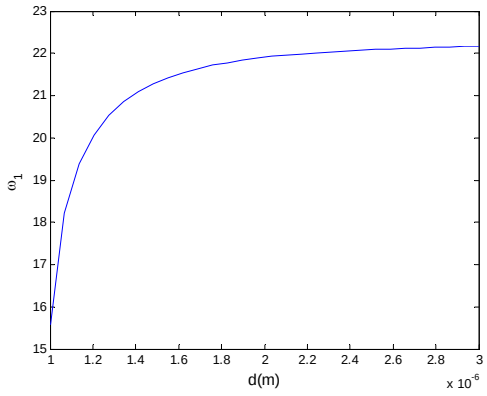
ACKNOWLEDGMENTS

The authors thanks to all those who help us to improve the quality of the manuscript.

https://doi.org/10.1017/jmech.2014.12 Published online by Cambridge University Press



(a)



(b)

Fig 10 Variations of the fundamental natural frequency with gap distance (a) $V_p = 2$ (b) $V_p = 10$

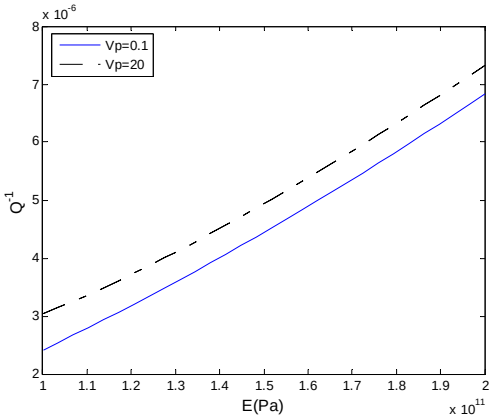


Fig. 11 Thermoelastic damping versus Young's modulus

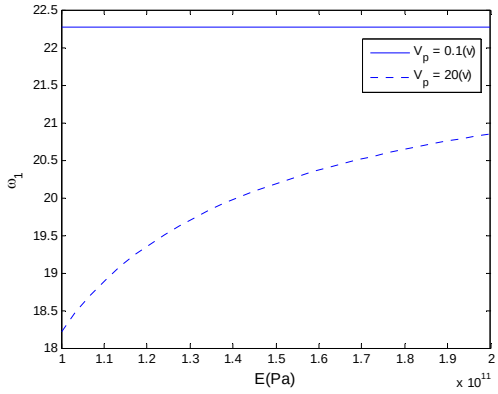


Fig. 12 Variations of the fundamental natural frequency with Young's modulus

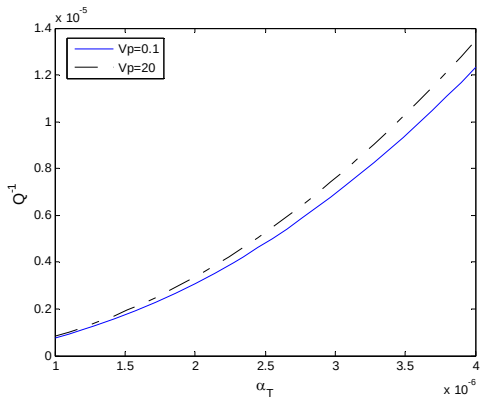


Fig. 13 Thermoelastic damping versus coefficient of thermal expansion

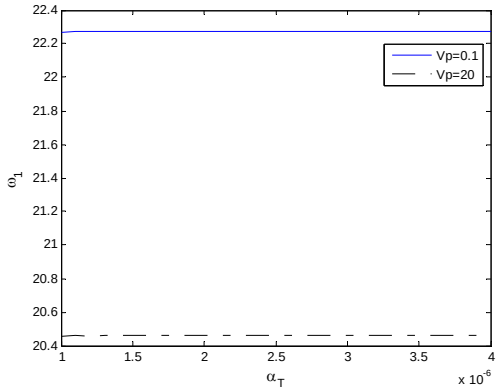


Fig. 14 Variations of the fundamental natural frequency with coefficient of thermal expansion

REFERENCES

1. Nayfeh, A. H. and Younis, M. I., "A New Approach to the Modeling and Simulation of Flexible Microstructures Under the Effect of Squeeze-Film Damping," *Journal of Micromechanics and Microengineering*, **14**, p. 170 (2004).
2. Nayfeh, A. H. and Younis, M. I., "Modeling and Simulations of Thermoelastic Damping in Microplates," *Journal of Micromechanics and Microengineering*, **14**, p. 1711 (2004).
3. Sun, Y. and Saka, M., "Thermoelastic Damping in Micro-Scale Circular Plate Resonators," *Journal of Sound and Vibration*, **329**, pp. 328–337, (2009).
4. Zener. C., "Internal Friction in Solids I. Theory of Internal Friction In Reeds," *Physical Review*, **52**, p. 230 (1937).
5. Zener, C., "Internal Friction in Solids II. General Theory of Thermoelastic Internal Friction," *Physical Review*, **53**, p. 90 (1937).
6. Alblas, J. B., "A Note on the Theory of Thermoelastic Damping," *Journal of Thermal Stresses*, **4**, pp. 333–355 (1981).
7. Lifshitz, R. and Roukes, M. L., "Thermoelastic Damping in Micro- and Nanomechanical Systems," *Physical Review B*, **B61**, p. 5600 (2000).
8. Sudipto, K. De and Aluru, N. R., "Theory of Ther-

https://doi.org/10.1017/jmech.2014.12 Published online by Cambridge University Press

moelastic Damping in Electrostatically Actuated Microstructures," *Physical Review B*, **B74**, p. 144305 (2006).
9. Prabhakar, S. and Vengallatore, S., "Theory of Thermoelastic Damping in Micromechanical Resonators with Two-Dimensional Heat Conduction," *Journal of Microelectromechanical Systems*, **17**, pp. 494–502 (2008).
10. Yi, Y. B. and Matin, M. A., "Eigenvalue Solution of Thermoelastic Damping in Beam Resonators Using a Finite Element Analysis," *Journal of Vibration and Acoustics*, **129**, pp. 478–483 (2007).
11. Serra, E. and Bonaldi, M., "A Finite Element Formulation for Thermoelastic Damping Analysis," *International Journal for Numerical Methods in Engineering*, **78**, pp. 671– 691 (2009).
12. Choi, J., Cho, M. and Rhim, J. "Efficient Prediction of the Quality Factors of Micromechanical Resonators," *Journal of Sound and Vibration*, **329**, pp. 84–95 (2010).
13. Guo, F. L. and Rogerson, G. A., "Thermoelastic Coupling Effect on a Micro-Machined Beam Resonator," *Mechanics Research Communications*, **30**, pp. 513–518 (2003).
14. Batra, R. C., Porfiri, M. and Spinello, D., "Review of Modeling Electrostatically Actuated Microelectromechanical Systems," *Smart Materials and Structures*, **12**, p. 759 (2007).
15. Abdel-Rahman, E. M., Younis, M. I. and Nayfeh, A. H., "Characterization of the Mechanical Behavior of an Electrically Actuated Microbeam," *Journal of Micromechanics and Microengineering*, **16**, pp. R23–R31 (2002).
16. Nayfeh, A. H. and Younis, M. I., "Dynamics of MEMS Resonators Under Superharmonic and Subharmonic Excitations," *Journal of Micromechanics and Microengineering*, **15**, p. 1810 (2005).
17. Younis, M. I. and Nayfeh, A. H., "A Study of the Nonlinear Response of a Resonant Microbeam to an Electric Actuation," *Nonlinear Dynamics*, **31**, pp. 91–117 (2003).
18. Younis, M. I., Abdel-Rahman, E. M. and Nayfeh, A. H., "A Reduced-Order Model for Electrically Actuated Microbeam-Based," *MEMS Journal of Micromechanics Systems*, **12**, pp. 672–680 (2003).
19. Abdel-Rahman, E. M. and Nayfeh, A. H., "Secondary Resonances of Electrically Actuated Resonant Microsensors," *Journal of Micromechanics and Microengineering*, **13**, p. 4917 (2003).
20. Nayfeh, A. H. and Younis, M. I., "Dynamics of MEMS Resonators Under Superharmonic and Subharmonic Excitations," *Journal of Micromechanics and Microengineering*, **15**, p. 1840 (2005).
21. Najar, F., Choura, S., Abdel-Rahman, E. M., El-Borgi, S. and Nayfeh, A. H., "Dynamic Analysis of Variable-Geometry Electrostatic Microactuators," *Journal of Micromechanics and Microengineering*, **16**, p. 2449 (2006).
22. Zhao, X., Abdel-Rahman, E. M. and Nayfeh, A. H., "A Reduced-Order Model for Electrically Actuated Microplates," *Journal of Micromechanics and Microengineering*, **14**, p. 900 (2004).
23. Vogl, G. W. and Nayfeh, A. H., "A Reduced-Order Model for Electrically Actuated Clamped Circular Plates," *Journal of Micromechanics and Microengineering*, **15**, p. 684 (2005).
24. Ouakad, H. M., and Younis, M. I., "The Dynamic Behavior of MEMS Arch Resonators Actuated Electrically," *International Journal of Non-Linear Mechanics*, **45**, pp. 704–713 (2010).
25. Batra, R. C., Porfiri, M. and Spinello, D., "Electromechanical Model of Electrically Actuated Narrow Microbeams," *Journal of Microelectromech*, **15**, pp. 1175–1189 (2006).
26. Fargas Marqu`es, A., Costa Castell´o, R. and Shkel, A. M., "Modelling the Electrostatic Actuation of MEMS: State of the Art 2005," *Technical Report*, *IOC-DT-P-2005-18*, p. 66 (2005).
27. Nayfeh, A. H. and Pai, P. F., *Linear and Nonlinear Structural Mechanics*, Wiley-Interscience, Hoboken, New Jersey, p. 763 (2004).
28. Süli, E. and Mayers, D. F., *An Introduction to Numerical Analysis*, Cambridge University Press, England, pp. 361–380 (2003).

(Manuscript received March 4, 2012,
accepted for publication May 14, 2013.)

https://doi.org/10.1017/jmech.2014.12 Published online by Cambridge University Press